Remote Sens. **2013**, *5*, 6921-6937; doi:10.3390/rs5126921

OPEN ACCESS

Remote Sensing

ISSN 2072-4292

www.mdpi.com/journal/remotesensing

Article

Block-to-Point Fine Registration in Terrestrial Laser Scanning

Jin Wang

Geodätisches Institut, Leibniz Universität Hannover, D-30167 Hannover, Germany;
E-Mail: wang@gih.uni-hannover.de; Tel.: +49-511-762-3584

Received: 23 October 2013; in revised form: 3 December 2013 / Accepted: 5 December 2013 / Published: 11 December 2013

Abstract: Fine registration of point clouds plays an important role in data analysis in Terrestrial Laser Scanning (TLS). This work proposes a block-to-point fine registration approach to correct the errors of point clouds from TLS and of geodetic networks observed using total stations. Based on a reference coordinate system, the block-to-point estimation is performed to obtain representative points. Then, fine registration with a six-parameter transformation is performed with the help of an Iterative Closest Point (ICP) method. For comparisons, fine registration with a seven-parameter transformation is introduced by applying a Singular Value Decomposition (SVD) algorithm. The proposed method not only corrects the registration errors between a geodetic network and the scans, but also considers the errors among the scans. The proposed method was tested on real TLS data of a dam surface, and the results showed that distance discrepancies of estimated representative points between scans were reduced by approximately 60%.

Keywords: terrestrial laser scanning; fine registration; block-to-point estimation; systematic errors

1. Introduction

Terrestrial Laser Scanning (TLS) is a powerful geodetic tool ideal for supporting a wide spectrum of applications in many different environments, e.g., [1,2]. Registration is a prerequisite in TLS data processing. In this paper, we present a fine registration approach, where after transforming all the scans into the reference coordinate system, point clouds are divided into small blocks, and then, each block is described by a representative point. Then, a rigid body movement and a similarity transformation are used to detect and correct the errors of representative points between two scans. An Iterative Closest Point (ICP) method is applied to estimate the six-parameter transformation, and a Singular Value

Decomposition (SVD) algorithm is used to estimate the seven-parameter transformation. The advantages of the proposed method mean that not only the registration errors from scans to the reference coordinate system are processed, but, also, the errors between the scans are considered.

Previous work about registration methods can be found in the following literature. A Least Squares 3D (LS3D) surface matching [3] utilizes a generalized Gauss–Markov (GM) model and minimizes the sum of the squares of Euclidean distances between two surfaces. The generalized GM model is composed of a GM estimation model and an extension model, where the unknown parameters are introduced as fictitious observations. Later, an integrated model [4], which considers simultaneously the match surface geometry and intensity information, was introduced. For the LS3D method, the discrete point cloud is represented as a patch-wise surface function [5]. The difference with other surface matching methods, such as a the Scale Invariant Feature Transform (SIFT) algorithm [6], is that the LS3D method worked based on the discrete point cloud, while the SIFT algorithm operated based on images. Although a point cloud from a TLS could be generated as an image, the operated datasets between these two methods are different. The presented approach follows closely on the usage of the point clouds from [7]. The patches defined from discrete point clouds were used as observations in a generalized GM model. Similarly, processing the points firstly, a fine registration of two range images was introduced by first aligning feature points, followed by feature surface elements, which are sets of points corresponding to the image area determined by the feature [8].

Recently, Grant *et al.* [9] presented a similar approach to [8]. Instead of any artificial targets, a point-to-plane approach was launched to register with a general least-squares adjustment method. The point-to-plane correspondence was formed from both scans. A point in a scan and the three nearest scanned points in the other scan constructed a transform point and a hypothesized corresponding planar element. Then, the point was transformed to the planar system. These researches mean that firstly processing the point clouds and then using registration methods may be a reasonable way to get more accurate registration results. An attempt was performed earlier in [10], where a fine registration was estimated with the help of the ICP method. However, there are still some errors existing in the datasets.

For TLS applied in structural monitoring tasks, a uniform framework needs to be established to describe the object surface and to compare the deformation of an object surface between different epochs. Object surfaces could be recognized in the following two methods: those that segment points based on criteria, like the proximity of points, and those that directly estimate surface parameters [11]. In many cases, the second type of method is suitable and convenient for regular object shapes, like ellipsoids and cylinders, which could be described by several parameters. Thus, in this paper, a quadratic form estimation [12,13] is used to describe the shape of the object surface and to establish a uniform framework (see Section 2.2).

Previous work for TLS applied in structural monitoring tasks was often performed in the following two steps (e.g., [14]). Point clouds are firstly transformed from multiple scans into a reference coordinate system. Then, the object surface is described by a mathematical model for epoch comparisons. However, the errors among different scanner stations were neglected. In order to adjust these errors, the fine registration is introduced. The basic idea of a transformation is to map a point or a feature in one coordinate system to a point or feature in another coordinate system. Many types of functions could be used to specify the mapping relationships: rigid body movement, similarity transformation, affine

transformation, and so on. In the field of TLS, the rigid body movement and the similarity transformation are typically applied for data transformations. The rigid body movement estimates six transformation parameters, which includes three rotations and three translations. If there is a scale difference between the scanner and the objects, the similarity transformation can be used (Vosselman and Maas [15]). For comparisons in this paper, the rigid body transformation and the similarity transformation are used and compared in the process of fine registration.

For the rigid body transformation, an ICP algorithm proposed by Besl and McKay [16] is commonly used to estimate the six transformation parameters in TLS data processing. A basic version of the ICP method is based on the search of pairs of nearest points in two datasets and, then, to estimate a rigid body movement. The ICP method runs the whole dataset directly in most of the applications (e.g., [14]), while the LS3D algorithm divides the whole dataset into patches firstly, then iterates to obtain the transformation parameters. At the same time, the ICP and its variant algorithms minimize the Euclidean distances between two point clouds by least-squares and indirectly estimate the rigid body movement, while the LS3D method directly formulates a GeneralizedGM model.

Under a similar assumption that both observations and a datum are contaminated by errors, a SVD algorithm can be used to compute similarity transformation parameters within an Errors-In-Variables (EIV) model [17], where the EIV model is a specific type of Gauss–Helmert model. In this case, no iteration and no initial values are necessary to solve the transformation parameters. This saves running time when there are thousands of representative points. For long distances between two scans, the seven-parameter transformation may be more suitable, due to estimating the scale factor. In general cases, the SVD algorithm itself can also be used to estimate the six transformation parameters, and the ICP method itself can also be used to estimate the seven transformation parameters. In this paper, the SVD algorithm is used in the fine registration with seven-parameter transformation; while the ICP method is used in the fine registration with six-parameter transformation. Both the two fine registration types can be employed in the proposed procedure, and their suitability will be compared with experimental data.

In the research demonstrated in this paper, the fine registration in TLS applications is processed by first transforming the point clouds into a reference coordinate system, followed by block-to-point estimation; then, the fine registration is performed based on the estimated representative points. The next section of this paper will present the proposed method. Section 3 displays a real application in a scanning task of a dam surface. The conclusion and future work are presented finally.

2. Proposed Method

In this paper, we present a new methodology that extends the work of Eling [14], Felus and Burtch [17] and Besl and McKay [16]. The result is expected to improve the quality of registration and to decrease or eliminate the effect of random and systematic errors between the scans in TLS applications. By block-to-point estimation, points in one block were estimated as a representative point, then six-parameter transformation is applied for fine registration; for comparisons, fine registration with seven-parameter transformation is also proposed. The proposed method processes the errors between different scanner stations, where these errors are neglected in the work of [14]. Fine registration is employed based on the estimated representative points, not on the original points. Artificial targets

are used to estimate the transformation parameters from scans to a local reference system, while the estimated representative points are used in the process of fine registration.

The proposed method is presented in three steps (Figure 1): Firstly, a combined model is used to transform all the scans to a reference coordinate system with the help of identical points. Secondly, a quadratic form estimation and a segmentation method are introduced to describe the object surface and then divide the object surface into small blocks based on point clouds from TLS. The point cloud in each block is estimated as a representative point. This step is also named block-to-point estimation. Thirdly, based on these representative points, the six-parameter transformation and the seven-parameter transformation are applied to adjust the errors of representative points between multiple scans with the help of the ICP method and the SVD algorithm, respectively. Figure 1 demonstrates the workflow of TLS applied in structural monitoring tasks. The registration errors between the network and the scans are processed in step 1. Then, the errors between the scanner stations are adjusted in step 3. It may be more reasonable and comprehensive to adjust the errors between the network and the scans by considering both these two groups of errors.

Figure 1. Data processing workflow of Terrestrial Laser Scanning (TLS) applied in structural monitoring tasks. ICP, Iterative Closest Point; SVD, Singular Value Decomposition.

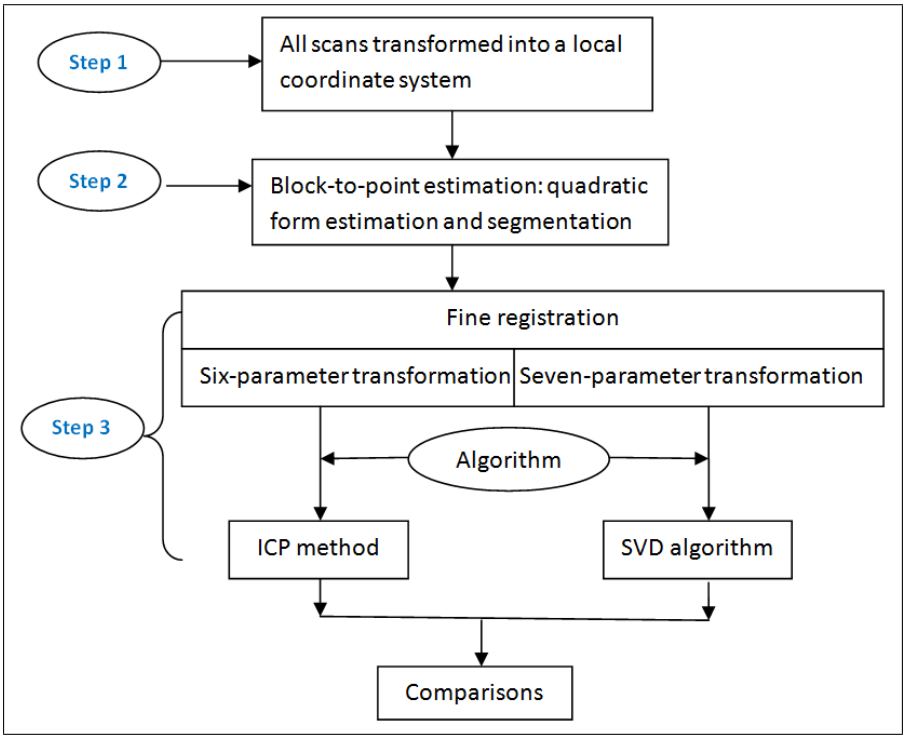

2.1. Transformation

To obtain a complete representation of an object surface, all the point clouds from two or more scans need to be transformed from their local scanner coordinate systems into a reference coordinate system, where the reference coordinate system can either be a local coordinate system or be a global coordinate system. The transformation parameters can be determined from identical points in both

coordinate systems. The similarity transformation of the coordinates from one coordinate system to another coordinate system is defined as:

$$\mathbf{Y}_j^i = \mathbf{\Delta X}^i + m^i \mathbf{R}^i \mathbf{X}_j^i \tag{1}$$

where $i = 1, 2, ..., s$; $j = 1, 2, ..., p$, s and p identify the total number of scanner stations and identical points, respectively, $\mathbf{Y}$ is the vector of the coordinates in the reference coordinate system, $\mathbf{X}$ is the vector of the coordinates in the scanner system, $\mathbf{\Delta X}$ is the vector of the translations of the scanner system, m is the scale and $\mathbf{R}$ is the rotation matrix with the three rotation angles (ω, ϕ, κ).

The unknown parameters could be solved by the iterative Gauss–Helmert model [18]. In this model, external parameters and transformation parameters are estimated simultaneously (for details, see [19]). Thereafter, all the point clouds can be transformed into the reference coordinate system.

If there are no systematic errors, the expected distance discrepancies between multiple scans would be zero. However, in practical applications, this is never the case. For example, as demonstrated by [14], systematic errors with a magnitude of approximately 5 mm were detected, even when the calibrations of the vertical angles and the distances were undertaken before the scanning process. Thus, considering errors between the multiple scans is reasonable and important.

2.2. Block-to-Point Estimation

The registration of point clouds could be achieved, e.g., by applying the ICP method [16]. However, the explicit point correspondence is hard to confirm, and this causes the lower precision of the registration. In order to compare the possible deformation of objects from different epochs, a uniform framework is established with the help of the estimated parameters of the quadratic form. A segmentation method is then used to divide the object surface into small blocks. In the research presented in this paper, these two steps, named block-to-point estimation, are used to estimate representative points. These points establish explicit correspondences between the two datasets. After that, instead of the original point clouds, the representative points are used to describe the object surface.

A quadratic form could be used by evaluation of determinants and then testing the form parameters to describe the object surface [12,13]. The equation for a quadratic form estimation can be written by:

$$a_1 x_k^2 + a_2 y_k^2 + a_3 z_k^2 + 2a_4 x_k y_k + 2a_5 x_k z_k + 2a_6 y_k z_k + a_7 x_k + a_8 y_k + a_9 z_k + a_{10} = 0 \tag{2}$$

where $\mathbf{x}_k$ is the coordinate vector of a single point and $k = 1, 2..., n$, n denotes the total number of points scanned by TLS. The parameters, a_i, could also be expressed as:

$$\mathbf{x}_k = \begin{pmatrix} x_k \\ y_k \\ z_k \end{pmatrix}, \quad \mathbf{M} = \begin{pmatrix} a_1 & a_4 & a_5 \\ a_4 & a_2 & a_6 \\ a_5 & a_6 & a_3 \end{pmatrix}, \quad \mathbf{m} = \begin{pmatrix} a_7 \\ a_8 \\ a_9 \end{pmatrix} \quad \text{and} \quad \alpha = a_{10} \tag{3}$$

where $i = 1, 2, ...10$, $\mathbf{M}$ is the 3×3 symmetric coefficient matrix, $\mathbf{m}$ is the coefficient vector and α is the scalar.

The parameters from a_1 to a_{10} could be estimated by a Gauss–Helmert model with several steps of iteration for convergence. To avoid repeating, details are in [13]. A determinant method, in which an

extended form matrix $\mathbf{M}^*$ is constructed, is used to estimate the four motion invariant parameters, δ, Δ, B and J [12].

The extended form matrix is identified:

$$\mathbf{M}^* = \begin{pmatrix} \mathbf{M} & \mathbf{m} \\ \mathbf{m}^T & a_{10} \end{pmatrix} \tag{4}$$

The functions of the four parameters, δ, Δ, B and J, could be generated as follows:

$$\begin{aligned} \delta &= det(\mathbf{M}^*), \quad \Delta = det(\mathbf{M}) \\ B &= det(\mathbf{M}_1^*) + det(\mathbf{M}_2^*) + det(\mathbf{M}_3^*) \\ J &= det(\mathbf{M}_1) + det(\mathbf{M}_2) + det(\mathbf{M}_3) \end{aligned} \tag{5}$$

The shape of the object surface may be determined by looking for the test tree of automatic form recognition [12]. The advantage of this method is that only several parameters need to be estimated to describe the shape of the object surface.

Based on the estimated parameters of quadratic form estimation, the segmentation is performed in a spherical coordinate system according to the horizontal angles and the vertical angles. The coordinates, $\mathbf{x}(p_u, q_v)$, of the block centers can be derived by:

$$\mathbf{x}(p_u, q_v) = \begin{pmatrix} x(p_u, q_v) \\ y(p_u, q_v) \\ z(p_u, q_v) \end{pmatrix} \tag{6}$$

where p_u and q_v are defined according to the size of the block, with:

$$\begin{aligned} \mathbf{p}^T &= [p_1, p_2, ..., p_m], \quad \text{with} : p_{u+1} = p_u + \Delta p, \quad u = 1, 2, ..., m \\ \mathbf{q}^T &= [q_1, q_2, ..., q_n], \quad \text{with} : q_{v+1} = q_v + \Delta q, \quad v = 1, 2, ..., n \end{aligned} \tag{7}$$

where m and n are the total numbers of rows and columns of the whole framework, Δp and Δq are the intervals of neighboring blocks in the vertical direction and the horizontal direction, respectively. The first block starts from the right bottom of the object surface.

According to the point clouds in a block, the least-squares method is used to estimate the representative point in this block. Because both the block size and curvature of the block surface are small, the point clouds in one block usually are distributed on a plane surface. Thus, the normal vectors, $\mathbf{n}$, and the distance, d, of a block are defined to evaluate the plane surface:

$$\hat{\mathbf{n}}^T \cdot \mathbf{x}_k + \hat{d} = 0 \quad \text{with} : \quad \hat{\mathbf{n}}^T = [\hat{n}_x, \hat{n}_y, \hat{n}_z], \quad \mathbf{x}_k^T = [x_k, y_k, z_k], \quad k = 1, 2, ..., w \tag{8}$$

where w is the number of points in a block. The covariance matrix, $\hat{\mathbf{\Sigma}}_{\hat{b}}$, includes the stochastic information of the estimated parameters and is estimated with the eigenvalues and eigenvectors of the points in a block:

$$\hat{\mathbf{\Sigma}}_{\hat{b}} = \hat{\sigma}_0^2 \begin{pmatrix} \mathbf{Q}_{\hat{\mathbf{n}}\hat{\mathbf{n}}} & \mathbf{0} \\ \mathbf{0} & \mathbf{q}_{\hat{d}\hat{d}} \end{pmatrix} \tag{9}$$

The center point, $\mathbf{x}_{bc}$, of the block is introduced to estimate the representative point, $\hat{\mathbf{x}}_r$:

$$\hat{\mathbf{x}}_r = \mathbf{x}_{bc} + (\hat{d} - \hat{\mathbf{n}}^T \mathbf{x}_{bc})\hat{\mathbf{n}}, \quad \text{with} \quad |\hat{\mathbf{n}}| = 1 \tag{10}$$

A differential function of $\hat{\mathbf{n}}$ and $\hat{d}$ in Equation (10) is expressed by a matrix, $\mathbf{D}$:

$$\mathbf{D} = \begin{pmatrix} \hat{d}-2\hat{n}_x x_{bc}-\hat{n}_y y_{bc}-\hat{n}_z z_{bc} & -\hat{n}_x y_{bc} & -\hat{n}_x z_{bc} & \hat{n}_x \\ -\hat{n}_y x_{bc} & \hat{d}-\hat{n}_x x_{bc}-2\hat{n}_y y_{bc}-\hat{n}_z z_{bc} & -\hat{n}_y z_{bc} & \hat{n}_y \\ -\hat{n}_z x_{bc} & -\hat{n}_z y_{bc} & \hat{d}-\hat{n}_x x_{bc}-\hat{n}_y y_{bc}-2\hat{n}_z z_{bc} & \hat{n}_z \end{pmatrix} \tag{11}$$

By means of the variance propagation algorithm, the covariance matrix, $\mathbf{\Sigma}_{\hat{\mathbf{x}}_r\hat{\mathbf{x}}_r}$, of the representative points, $\hat{\mathbf{x}}_r$, is given by:

$$\hat{\mathbf{\Sigma}}_{\hat{\mathbf{x}}_r\hat{\mathbf{x}}_r} = \mathbf{D} \cdot \hat{\mathbf{\Sigma}}_{\hat{b}} \cdot \mathbf{D}^T \tag{12}$$

Thereafter, with the block-to-point estimation, the representative points are prepared to describe the object surface.

2.3. Fine Registration

In the transformation model in step 1, the registration errors between the scanner stations and the reference coordinate system are adjusted, but the errors among the multiple scans are not included. In order to detect and decrease the distance discrepancies among these multiple scans, a rigid body movement and a similarity transformation are used. The ICP method is commonly used to estimate the rigid body movement parameters. For a comparison with the rigid body movement, the similarity transformation is applied with the help of the SVD algorithm.

Figure 2. Block-to-point correspondence in fine registration. The red points are the estimated representative points of blocks $\mathbf{X}_1$ and $\mathbf{X}_2$, where these two blocks are from two different scans. ($\mathbf{X}$, $\mathbf{Y}$, $\mathbf{Z}$) denotes the reference coordinate system. If there are no systematic or random errors, the distances between these two red points could be zero. However, they are always errors in real cases.

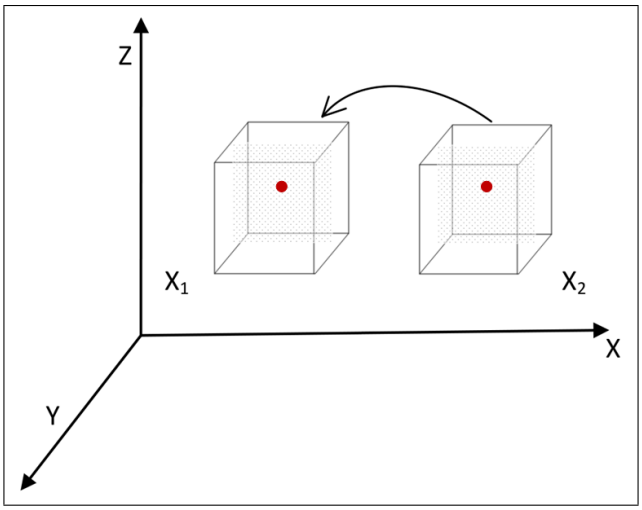

The red points in Figure 2 are the estimated representative point correspondence of two blocks from two scan datasets, $\mathbf{X}_1$ and $\mathbf{X}_2$. If there are no systematic or random errors, the distance discrepancy between these two representative points would be zero. In order to adjust this kind of error, fine registration is proposed either with the help of the six-parameter transformation or with the help of

the seven-parameter transformation (see step 3 in Figure 1). The ICP method estimates six parameters (three translations and three rotations), while the SVD algorithm estimates seven parameters (three translations, three rotations and one scale). The performance of each of the algorithms depends on the quality of observations and the measurement environment. If the scale factor is important in a given case, seven-parameter transformation would perform better in the processing of fine registration. Otherwise, if the distances among the scans and the object surface are quite close to each other, the scale factor may be insignificant.

2.3.1. Fine Registration with Six-Parameter Transformation

In the process of the ICP method, one of the datasets is considered as a reference coordinate system. The other dataset is moved to the reference coordinate system. The rigid body movement function can be generally expressed as [15]:

$$\mathbf{X}_1 = \mathbf{R}_I \mathbf{X}_2 + \Delta \mathbf{X}_I \tag{13}$$

where $\mathbf{R}_I$ is the rotation matrix, $\Delta \mathbf{X}_I$ is the translation vector and $\mathbf{X}_2$ and $\mathbf{X}_1$ are the moving and the reference point sets, respectively. When the two datasets converge, corrections of the resulting rigid body movement become smaller during iteration, and a solution iteratively approaches a global minimum. The minimum distance, D, could be written as:

$$D = \sum \| \mathbf{X}_2 - \mathbf{X}_1 \|^2 \tag{14}$$

where $\| \cdot \|$ denotes the length of the vector.

Two aspects should be concerned when the ICP method is applied: computation time and proper initial values. Two strategies were employed to speed up the computation time and improve data quality: (1) reduction of the number of the matching points through the quadratic form estimation; and (2) speeding up the accuracy of the datasets by providing proper initial values.

One issue in applying the ICP algorithm is that it requires proper initial approximations for convergence to the local minimum. With the introduction of block-to-point estimation, good initial values could be obtained. Another issue occurs when two data regions overlap. Adopting the quadratic form estimation and segmentation methods throws out the points that are unique to each dataset. This means the remaining points are only those that are visible in both scans and have correspondences. Therefore, the two datasets iterated in the ICP algorithm are entirely overlapping regions. This means that the distance discrepancies existing between the scanner stations may be decreased. Note that in [14,20], the applications of ICP method were based on original point clouds, while in the research presented in this paper, the ICP method is applied based on the representative points.

2.3.2. Fine Registration with Seven-Parameter Transformation

For a comparison with the six-parameter transformation, the seven-parameter transformation is estimated by using the SVD algorithm. A standard algorithm (see Algorithm 3 in [17]) was performed to test the distance discrepancies of the representative points between two scans. The SVD algorithm is a factorization of a matrix, basically; here, it is used to compute the optimal parameters of the similarity transformation in an EIV model. The SVD algorithm could be illustrated as follows [17]:

1. Setting $\mathbf{B} = \mathbf{I}_n - \frac{\mathbf{1}_n \mathbf{1}_n^T}{n}$, where n is the number of the identical points, the center coordinates of the observations could be written as:

$$\bar{\mathbf{X}}_2 = \mathbf{B}\mathbf{X}_2, \quad \bar{\mathbf{X}}_1 = \mathbf{B}\mathbf{X}_1 \tag{15}$$

where $\bar{\mathbf{X}}_1$ and $\bar{\mathbf{X}}_2$ are the center coordinates of the observations, $\mathbf{X}_1$ and $\mathbf{X}_2$, from two coordinate systems, respectively. These observations are chosen as identical points in the process of fine registration. Then, $[\mathbf{U}, \mathbf{\Sigma}, \mathbf{V}] = svd\ (\bar{\mathbf{X}}_2^T \bar{\mathbf{X}}_1)$ produces a diagonal matrix, $\mathbf{\Sigma}$, with nonnegative diagonal elements in decreasing order, and unitary matrices, $\mathbf{U}$ and $\mathbf{V}$, so that:

$$\bar{\mathbf{X}}_2^T \bar{\mathbf{X}}_1 = \mathbf{U}\mathbf{\Sigma}\mathbf{V}^T \tag{16}$$

2. Setting $\mathbf{D} = \mathrm{diag}(1, 1, \det(\mathbf{U}\mathbf{V}^T))$, the estimated rotation matrix $\hat{\mathbf{R}}_s$ could be expressed by:

$$\hat{\mathbf{R}}_s = \mathbf{U}\mathbf{D}\mathbf{V}^T \tag{17}$$

3. The scale, $\hat{s}_s$, could be solved by:

$$\hat{s}_s = -\frac{b - \sqrt{(b^2 + 4a^2)}}{2a} \tag{18}$$

where a and b are the traces of the matrices, $(\bar{\mathbf{X}}_1^T \bar{\mathbf{X}}_2 \hat{\mathbf{R}}_s)$ and $(\bar{\mathbf{X}}_2^T \bar{\mathbf{X}}_2 - \bar{\mathbf{X}}_1^T \bar{\mathbf{X}}_1)$, respectively.

4. The translation vector $\Delta\hat{\mathbf{x}}_s$ is finally calculated by:

$$\Delta\hat{\mathbf{x}}_s = (\frac{1}{n} \times \mathbf{1}_n^T)(\mathbf{X}_1 - \mathbf{X}_2 \hat{\mathbf{R}}_s \hat{s}_s) \tag{19}$$

At the same time, the vector of the residuals of the configuration matrix and the observations could also be obtained.

The observations could either be corresponding points or be corresponding patches. The significant difference of the six-parameter transformation and the seven-parameter transformation in this paper lies especially in the estimation of the scale factor. Note that the performance of the ICP method and SVD algorithm introduced in this paper does not imply the abilities of the algorithms themselves, but rather, their corresponding fine registration patterns: the rigid body movement and the similarity transformation, respectively. In the step of fine registration, the magnitudes of errors between the scans are small, because in step 1, a good quality of transformation parameters has been obtained.

3. Application

3.1. Data Collection and Network Configuration

Four epochs of data were measured by [14] with a Trimble GX3D scanner over two years on the Oker dam surface (Figure 3A,B). A Leica TCA2003 total station was used to measure artificial targets. The scanner was used for scanning both the artificial targets and the dam surface. In each epoch, four scanner stations (station 1000, 2000, 3000 and 4000) were set up in front of the dam surface (Figure 3C).

Because the scanner station 3000 has only scanned part of the dam surface, point clouds from this scan were excluded in the following data processing. Backsight targets and identical points were applied for fixing the local geodetic network. The transformation parameters were solved with the method explained in Section 2.1; thus, all the points were transformed into this local reference coordinate system.

Figure 3. (**A**) Location map of the Oker dam in Germany. The red triangle is the location of the dam. (**B**) Photograph of the Oker dam surface. (**C**) Geodetic monitoring network of the Oker dam [14] (top view). The blue points are the scan positions.

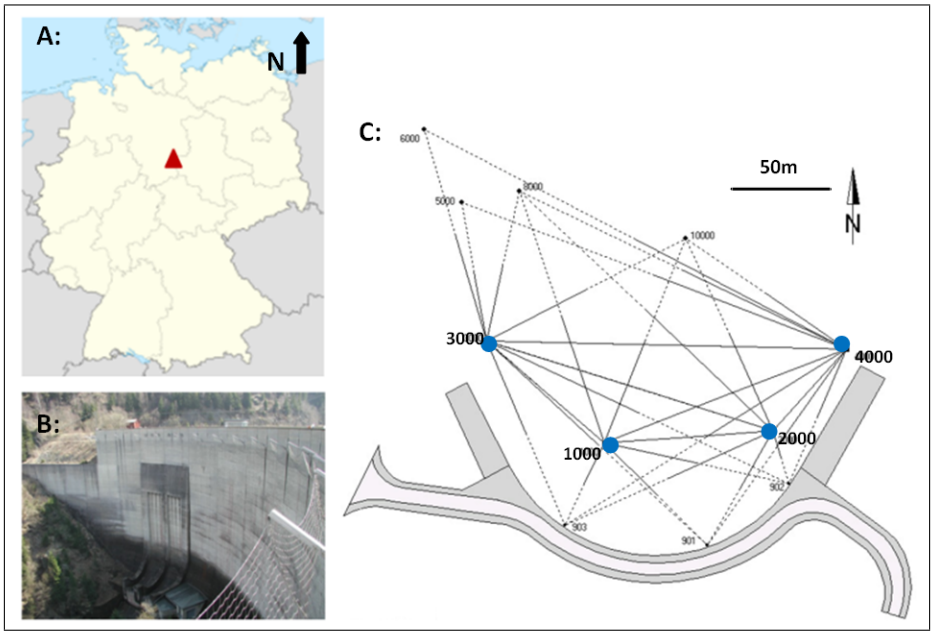

3.2. Block-to-Point Estimation

According to the quadratic form estimation, the object surface was estimated as an elliptical cylinder (Figure 4). Estimates of the elliptical cylinder are shown in Table 1, where $(\hat{x}_c, \hat{y}_c, \hat{z}_c)$ is the estimated center coordinate of the elliptical cylinder, z_c is the minimum value of the point clouds in the direction of z and $\hat{a}$ and $\hat{b}$ are the half-axes of the elliptical cylinder.

Based on the estimated parameters of the elliptical cylinder, rectangular blocks with small sizes were obtained according to the horizontal angles and the vertical angles of the point clouds. Points in one block were estimated as a representative point. Approximately $12,000$ blocks were segmented on the dam surface. The size of a block is shown in Table 2, where the depth of the block reliably excludes the points with large errors.

Similarly stated by [21], a proper block size should be carefully chosen. If the block is too large or if there is significant curvature in the block surface, smaller deformations of the block surface could be hard to detect by comparisons of the estimated representative points; if the block is too small, not enough of the points would be assigned to the block for estimating the representative point. The configuration of points in a block also influences the quality of the estimated representative point. The representative point, estimated from evenly distributed points in a block, is more reliable than the representative point obtained from unevenly distributed points.

Figure 4. Elliptic cylinder fitting. $(\mathbf{X_r}, \mathbf{Y_r}, \mathbf{Z_r})$ denotes the reference coordinate system. (x_c, y_c, z_c) denotes the center of the elliptic cylinder system, $(\mathbf{X_e}, \mathbf{Y_e}, \mathbf{Z_e})$. The red areas are the registered point clouds. The blue section is the fitted elliptic cylinder. The green point situated on the right bottom of the red section was the starting point of the segmentation.

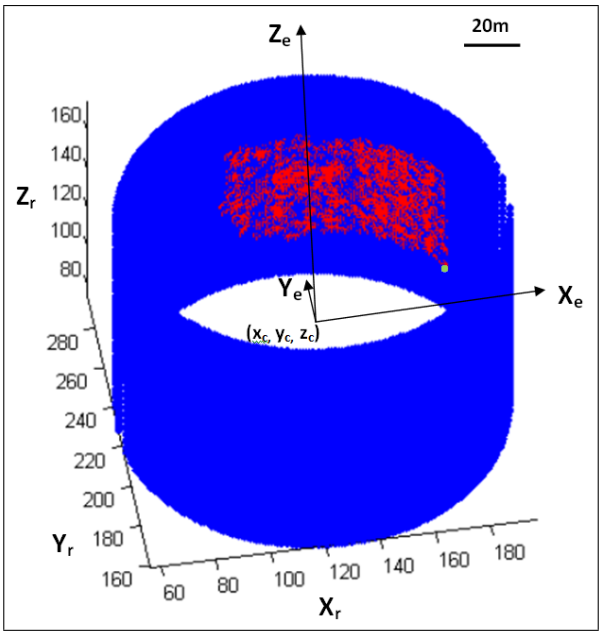

Table 1. The estimated parameters of the elliptical cylinder (m).

Estimated Parameters	$\hat{x}_c$	$\hat{y}_c$	z_c	$\hat{a}$	$\hat{b}$
Values	127.25	227.53	98.06	69.18	68.95

Table 2. The size of a block.

Size Of Block	**Width**	**Height**	**Depth**	**Width · Height**
Values	0.34 m	0.79 m	0.25 m	0.27 m^2

3.3. Fine Registration

Setting station 1000 as a reference station, the six-parameter transformation and the seven-parameter transformation are applied, respectively, to detect and decrease the distance discrepancies of representative points between two scans. The distance discrepancy, ds, of representative points could be calculated by:

$$ds = \sqrt{(\hat{x}'_r - \hat{x}''_r)^2 + (\hat{y}'_r - \hat{y}''_r)^2 + (\hat{z}'_r - \hat{z}''_r)^2} \tag{20}$$

where $(\hat{x}'_r, \hat{y}'_r, \hat{z}'_r)$ are the coordinates of the representative points from one scan and $(\hat{x}''_r, \hat{y}''_r, \hat{z}''_r)$ are the coordinates of the representative points from the second scan. If the distance from the representative

point to the elliptical cylinder center in the first scan is larger than that of the distance in the second scan, the value of the distance discrepancy is set as a positive number; otherwise, it is set as a negative number.

Under the same data sources, mean standard deviations of distance discrepancies of representative points in the four epochs are demonstrated in three groups: the results from [14]; the results from fine registration with six-parameter transformation; and the results from fine registration with seven-parameter transformation (Table 3). Due to the large difference in the standard deviations, a model chosen strategy to test additional parameters for significance is not carried out here.

Table 3. The mean standard deviation of distance discrepancies of representative points in the four epochs (the second column result comes from [14] without fine registration; "six-parameter transformation" means the result from fine registration with the ICP method; and " seven-parameter transformation" means the result from fine registration with the help of the SVD algorithm).

Mean Standard Deviation	Eling (2009)	Six-Parameter Transformation	Seven-Parameter Transformation
$\bar{ds}$	5 mm	3.2 mm	1.8 mm

In order to show more detail, Table 4 demonstrates the mean standard deviations ($\hat{\sigma}^1_{ds}$, $\hat{\sigma}^2_{ds}$ and $\hat{\sigma}^3_{ds}$) and the mean values ($\bar{ds}_2$ and $\bar{ds}_3$) of the distance discrepancies of representative points in epoch 4. The three groups are from the results of [14], where no fine registration, the fine registration with six-parameter transformation, as well as the fine registration with seven-parameter transformation were performed. The analysis of Tables 3 and 4 are shown in the following subsections.

Table 4. The mean standard deviations and the mean values of the distance discrepancies of representative points between two scans in epoch 4 ($\hat{\sigma}^1_{ds}$, $\hat{\sigma}^2_{ds}$ and $\hat{\sigma}^3_{ds}$ are the mean standard deviations from [14] without fine registration, fine registration using six-parameter transformation and fine registration using seven-parameter transformation, respectively; $\bar{ds}_2$ and $\bar{ds}_3$ are the mean values from fine registration using the six- and the seven-parameter transformation, respectively).

Epoch 4	$\hat{\sigma}^1_{ds}$ (Eling 2009)	$\hat{\sigma}^2_{ds}/\bar{ds}_2$ (with Six Parameters)	$\hat{\sigma}^3_{ds}/\bar{ds}_3$ (with Seven Parameters)
2000 to 1000	6.0 mm	2.92 mm/0.09 mm	1.62 mm/−0.09 mm
4000 to 1000	4.6 mm	3.43 mm/−0.09 mm	1.82 mm/0.35 mm
4000 to 2000	4.1 mm	3.70 mm/−1.61 mm	2.23 mm /0.14 mm

3.3.1. Fine Registration: Six-Parameter Transformation

The fine registration with six-parameter transformation was performed with the help of the ICP method in the four epochs. Setting station 1000 as the reference coordinate system, the representative points from station 2000 and station 4000 were transformed into this reference coordinate system. Under

the same data source, the mean standard deviation of distance discrepancies is approximately 3.2 mm with the six-parameter transformation (see Table 3). Comparing the systematic errors with a magnitude up to 5 mm without fine registration, the distance discrepancy was reduced approximately by 1.8 mm.

Figure 5 displays the variations of distance discrepancies in the corresponding representative points between two scans in epoch 4. The comparisons were demonstrated among station 1000 *vs*. station 2000, station 1000 *vs*. station 4000 and station 2000 *vs*. station 4000. The middle part of the dam surface is the most stable area; meanwhile, the largest biases happen in the boundary of the dam surface. For station 1000 *vs*. 2000, the distance differences vary from 0 mm to 12 mm, and the largest variation appears on the top right part of the dam surface. The most obvious variation occurs at the bottom of the dam surface in station 1000 *vs*. 4000. This is because station 4000 is the furthest scan away from the dam surface and longer distances have direct effects on the scanner's performance. Additionally, the coordinates in the transformation are with respect to the center of the dam surface, so the distance discrepancies in the center should be less than that of the boundary. One can also see that some systematic errors still exist in vertical directions in comparison with station 1000 *vs*. 4000, mainly due to the incomplete calibration and network configuration.

Figure 5. Distance discrepancies of representative points between two scans in epoch 4 (fine registration with six-parameter transformation)(mm) (the left figure means the variations of distance discrepancies between station 1000 and station 2000; the middle one is the variations of distance discrepancies between station 1000 and station 4000; the right figure denotes the variations of distance discrepancies between station 2000 and station 4000).

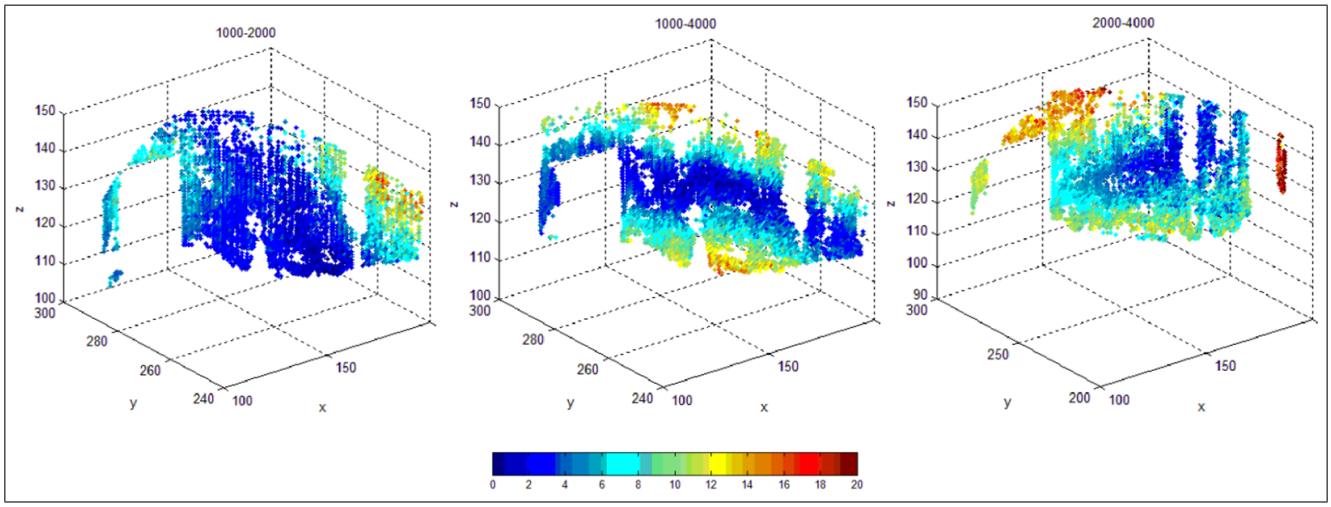

Table 4 and Figure 5 illustrate that the systematic errors are correlated with distances. The fine registration with six-parameter transformation certainly reduces the distance discrepancies of representative points between two scans, but some systematic errors still exist in the boundary of the dam surface. Eling's analysis [14] also showed that the systematic errors might be from the distances and the configuration of the network.

In many research projects (e.g., [14]), the ICP method was performed directly based on the original point clouds; whereas, the ICP method here was applied based on the representative points. This does not only reduce that data volume, but also, it provides the explicit correspondences between two datasets.

3.3.2. Fine Registration: Seven-Parameter Transformation

Fine registration with seven-parameter transformation was performed for the comparison with the six-parameter transformation. In Tables 3 and 4, the mean standard deviation of the distance discrepancies of representative points is approximately 1.8 mm in the four epochs; while the mean values of distance discrepancies are close to zero. In the case of transforming data from station 4000 to 1000 and from station 2000 to 1000, the mean standard deviations and mean values of distance discrepancies decreased faster than the transformation from station 4000 to 2000, because the distances from station 4000 to 1000 and from station 2000 to 1000 are longer than the distances from station 4000 to 2000 (see Figure 3). The mean standard deviations and the mean values of the distance discrepancies of representative points between the scans are smallest in the fine registration with seven-parameter transformation.

Figure 6. Distance discrepancies of representative points between two scans in epoch 4 (fine registration with seven-parameter transformation)(mm) (the left figure means the variations of distance discrepancies between station 1000 and station 2000; the middle one is the variations of distance discrepancies between station 1000 and station 4000; the right figure denotes the variations of distance discrepancies between station 2000 and station 4000).

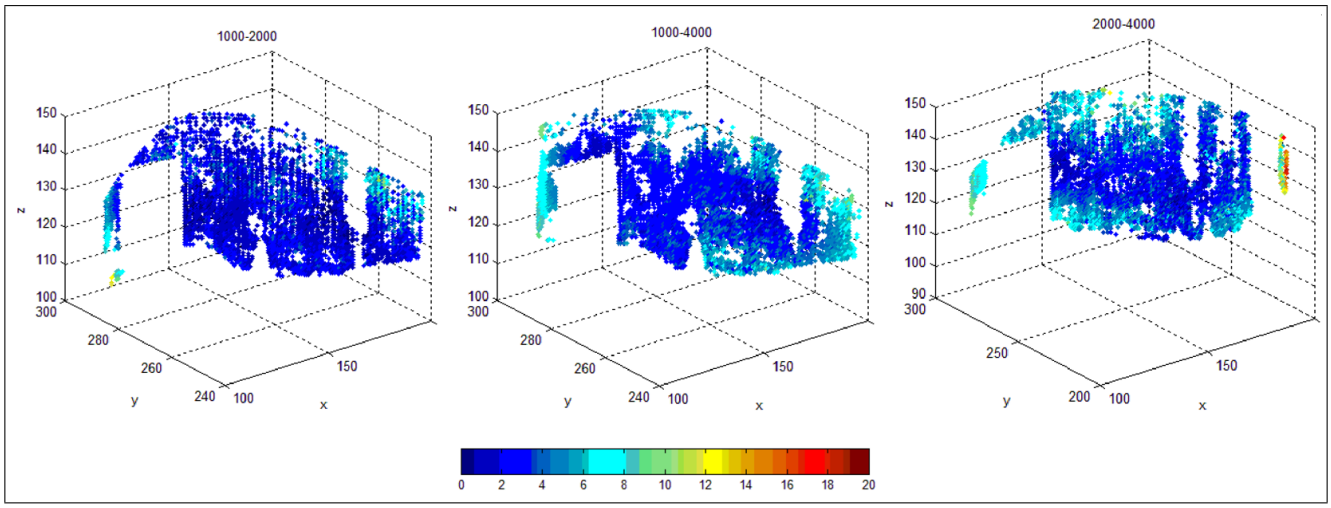

Figure 6 illustrates the variation of distance discrepancies of representative points between two scans. The variations of the center parts of the representative points are in the range of 0 mm to 5 mm. The distance discrepancies surrounding the dam surface vary more greatly than that of the center areas in each of the comparisons, because the center of the dam surface was scanned by each of the scans, but the surrounding areas were only scanned from certain scanner stations. The center areas have the highest density of point clouds for computation, while the areas around the outer parts of the dam surface have a lower density of point clouds. The same variation trend also appeared in the fine registration with six-parameter transformation, but with the seven-parameter transformation, the variation trend slows down. The fine registration with six-parameter transformation appeared as a systematic trend in vertical directions, while for the fine registration with seven-parameter transformation, the systematic trend decreased.

3.3.3. Discussion

In fine registration, the rigid body movement estimated six parameters by applying the ICP method, while for comparisons, the similarity transformation obtained seven parameters by applying the SVD algorithm. The mean standard deviation of distance discrepancies between the scans was decreased by approximately 3.2 mm based on the comparison between seven-parameter fine registration and [14]. This means that the systematic errors were decreased by approximately 60%. For shorter distances (e.g., from 5 m to 10 m), the rigid body movement and the similarity transformation get almost the same results, because the scale factor is not significant at such short distances. The scale factor from station 4000 to 1000 is approximately 1.000041, which means that for a 100-m distance, the scale has an effect with a magnitude of approximately 4.1 mm. This might explain why the seven-parameter transformation corrected the distance discrepancies of representative points better than that of the six-parameter transformation. Additionally, in step 1 in the workflow of Figure 1, if the calibration models were perfect, the scale factor would have less influence in this fine registration step. Because this paper focuses on fine registration, the calibration models are not demonstrated (see [19]).

As demonstrated in Tables 3 and 4, the proposed fine registration transformations show their ability in adjusting the distance discrepancies between multiple scans. If the distances from the scans to the object surface are longer than the distances in this application, the fine registration with seven-parameter transformation would be expected to be more important than that of the six-parameter transformation. Even with the introduction of fine registration, systematic errors with a magnitude of approximately 1.8 mm still exist in the datasets in this application. More identical points and a combination of internal and external calibration may be helpful in correcting the systematic errors.

Instead of the original point clouds, the computation based on the estimated representative points saves much time. For example, transforming the estimated points from station 2000 to station 1000 takes just under 10 s. The 10 s include the time of searching the explicit representative points and computing the parameters of fine registration. Users who have a high demand for data quality may perform this fine registration step.

For TLS applications, the estimated representative points could be compared in order to test if the corresponding points have significant variations in different epochs. Additionally, the deformation of the object is usually small; thus, the detection and elimination of these systematic errors are indispensable in the task of deformation monitoring, such as a water dam.

4. Conclusions and Future Work

This paper was focused on block-to-point fine registration in Terrestrial Laser Scanning (TLS), which is used for combined evaluation of point clouds from TLS and of geodetic networks observed using total stations. Of specific interest were those methods that utilize corresponding representative points, as they employ the original point clouds for registration (e.g., [14]). The block-to-point fine registration approach applies the quadratic form estimation and segmentation methods to guarantee the explicitly corresponding representative points between the scans. Thereafter, the six-parameter transformation was performed for fine registration to correct the distance discrepancies of representative points between the scans by applying the Iterative Closest Point (ICP) method. For comparisons, fine registration with

seven-parameter transformation was also applied with the help of the Singular Value Decomposition (SVD) algorithm.

Comparing fine registration with the six-parameter transformation and with the seven-parameter transformation, the seven-parameter transformation worked better, mainly due to the scale factor. Not only the registration errors from the scans to the reference coordinate system were considered, but also the distance discrepancies between the scans were treated. This is meaningful in real applications. In this paper with real TLS data from the Oker dam surface, the mean standard deviation of the distance discrepancies between the scans was decreased by approximately 3.2 mm based on the comparison between seven-parameter fine registration and [14]. This means that the systematic errors were decreased by approximately 60%.

The proposed block-to-point fine registration can be used in applications for objects with regular shapes. For complicated object surfaces that cannot be described by several parameters, other modeling methods are suggested to describe the object surfaces, such as the Non-Uniform Rational B-Spline (NURBS) model. Future work will try to apply the proposed method to other applications, such as tunnel monitoring tasks.

Acknowledgments

The work presented in this paper was conducted during my doctoral studies. I am grateful to Hansjörg Kutterer and Ingo Neumann for their guidance and helpful comments. The author would also like to thank Xing Fang for his help and discussion and Dirk Eling for providing the source data.

Conflict of Interest

The author declares no conflict of interest.

References

1. Barnhart, T.B.; Crosby, B.T. Comparing two methods of surface change detection on an evolving thermokarst using high-temporal-frequency terrestrial laser scanning, Selawik River, Alaska. *Remote Sens.* **2013**, *5*, 2813–2837.
2. Pesci, A.; Teza, G.; Bonali, E. Terrestrial laser scanner resolution: Numerical simulations and experiments on spatial sampling optimization. *Remote Sens.* **2011**, *3*, 167–184.
3. Gruen, A.; Akca, D. Least squares 3D surface and curve matching. *ISPRS J. Photogramm. Remote Sens.* **2005**, *59*, 151–174.
4. Akca, D. Matching of 3D surfaces and their intensities. *ISPRS J. Photogramm. Remote Sens.* **2007**, *62*, 112–121.
5. Wendt, A.; Heipke, C. A Concept for the Simultaneous Orientation of Brightness and Range Images. In Proceedings of the International Workshop on Recording, Modeling and Visualization of Cultural Heritage, Ascona, Switzerland, 22–27 May 2005; p. 451.
6. Lowe, D. Distinctive image features from scale-invariant keypoints. *Int. J. Comput. Vision* **2004**, *60*, 91–110.

7. Akca, D.; Gruen, A. A Flexible Mathematical Model for Matching of 3D Surfaces and Attributes. In Proceedings of SPIE—The International Society for Optical Engineering, San Jose, CA, USA, 28 February 2005; pp. 184–195.
8. Bendels, G.; Degener, P.; Wahl, R.; Körtgen, M.; Klein, R. Image-Based Registration of 3D-range Data Using Feature Surface Elements. In Proceedings of the 5th International Symposium on Virtual Reality, Archaeology and Cultural Heritage (VAST), Oudenaarde, Belgium, 7–10 December 2004; Volume 4, pp. 115–124.
9. Grant, D.; Bethel, J.; Crawford, M. Point-to-plane registration of terrestrial laser scans. *ISPRS J. Photogramm. Remote Sens.* **2012**, *72*, 16–26.
10. Wang, J.; Kutterer, H.; Fang, X. On the detection of systematic errors in terrestrial laser scanning data. *J. Appl. Geod.* **2012**, *6*, 187–192.
11. Vosselman, G.; Gorte, B.; Sithole, G.; Rabbani, T. Recognising structure in laser scanner point clouds. *Int. Arch. Photogramm. Remote Sens. Spat. Inf. Sci.* **2004**, *46*, 33–38.
12. Kutterer, H.; Schön, S. Statistische analyse quadratischer formen. *AVN* **1999**, *10*, 322–330.
13. Hesse, C.; Kutterer, H. Automated form Recognition of Laser Scanned Deformable Objects. In Proceedings of the Geodetic Deformation Monitoring: From Geophysical to Engineering Roles, Jaen, Spain, 17–19 March 2006; pp. 103–111.
14. Eling, D. *Terrestrisches Laserscanning für die Bauwerksüberwachung*; Fachrichtung Geodäsie und Geoinformatik, Leibniz Universität: Hannover, Germany, 2009.
15. Vosselman, G.; Maas, H.G. *Airborne and Terrestrial Laser Scanning*; Whittles: Dunbeath, UK, 2010; Volume 318.
16. Besl, P.; McKay, N. A method for registration of 3-D shapes. *IEEE Trans. Pattern Anal. Mach. Intell.* **1992**, *14*, 239–256.
17. Felus, Y.; Burtch, R. On symmetrical three-dimensional datum conversion. *GPS Sol.* **2009**, *13*, 65–74.
18. Pope, A. Some Pitfalls to be Avoided in the Iterative Adjustment of Nonlinear Problems. In Proceedings of the 38th Annual Meeting, American Society of Photogrammetry, Washington, DC, USA, 12–17 May 1972; pp. 449–473.
19. Wang, J. *Towards Deformation Monitoring with Terrestrial Laser Scanning Based on External Calibration and Feature Matching Methods*; Fachrichtung Geodäsie und Geoinformatik, Leibniz Universität: Hannover, Germany, 2013.
20. Lindenbergh, R.; Pfeifer, N.; Rabbani, T. Accuracy Analysis of the Leica HDS3000 and Feasibility of Tunnel Deformation Monitoring. In Proceedings of the ISPRS Workshop Laser Scanning 2005, Enschede, The Netherlands, 12–14 September 2005; pp. 24–29.
21. Lindenbergh, R.; Uchanski, L.; Bucksch, A.; Van Gosliga, R. Structural monitoring of tunnels using terrestrial laser scanning. *Rep. Geod.* **2009**, *2*, 231–239.